공학석사 학위논문

Preparation of Dip-coated Electrochromic Thin Film and Its Application to Photoelectrochromic Systems

딥 코팅 방법으로 만든 전기변색 박막의
광전기변색 시스템으로의 적용

2014년 8월

서울대학교 대학원
공과대학 화학생물공학부
박 재 혁

Abstract

Preparation of Dip-coated Electrochromic Thin Film and Its Application to Photoelectrochromic Systems

Jae-Hyuk Park
School of Chemical & Biological Engineering
The Graduate School
Seoul National University

Electrochromic and photochromic materials with reversible transmittance in response to an applied voltage and illumination, respectively, are the most common materials for smart windows. An alternative, the photo-electrochromic cell (PECC) was first demonstrated in 1996. For PECC, coloration is attained by the photon-electron conversion with no need for external power sources.

In this study, tungsten oxide (WO_3) thin film was fabricated by the sol-gel method with film thickness control by repeated dip coating process.

Electrochemical analysis was conducted in a three electrode half-cell using a lithium-based electrolyte and an optical transmittance change in colored/bleached state could be shown by using He-Ne laser (λ =633 nm).

From a materials analysis perspective, WO_3 thin films fabricated by the sol-gel method showed better adhesion with FTO glass after the annealing process when compared with samples without annealing. In addition, WO_3 films with amorphous phases exhibited better electrochromic performance than crystalline WO_3 films and film thickness control was possible by repeated dip coating. These results suggest that these modifications would be advantageous when assessing the electrochromic performance. Consequently, the optimum thickness for the best electrochromic performance was decided for employing to photoelectrochromic systems.

After that, we fabricated two types of WO_3 employed PECC. One is a layered structure composed of dye-sensitized TiO_2 nanoparticle (NP) on the crystalline WO_3 electrochromic film as the photoanode and employed the Pt counter electrode as a photocathode. The other is a separated structure composed of amorphous or crystalline WO_3 electrochromic film electrode as a photocathode and dye-sensitized TiO_2 NP as a photoanode. In addition, we apply WO_3 thin film with different thickness at two types of PECCs for understanding the transmittance change tendency when illuminated with time on cell compared to that of solely electrochromic sytems.

UV-vis spectra measurement results showed the sample with a thinner film

of WO_3 and with amorphous phases in separated structure exhibited the best coloration switching kinetics compared with others over illumination time and absolute transmittance change value was also quite remarkable.

Furthermore, WO_3 thin film in separated structure exhibited faster optical transmittance switching kinetics with illumination time than that of in layered structure.

Consequently, this results show that WO_3 employed two type of the photoelectochromic system exhibited same tendency compared to crystalline phase and film thickness dependent electrochromic properties.

Lastly, for enhancing the optical properties of photoelectrochromic systems, which were dip-coated WO_3 electrochromic thin film was employed, more transparent dyes on TiO_2 NP have to be used for higher initial transmittance value (as-prepared state) in two types of photoelectrochromic systems.

Keywords: WO_3, Dip coating, Photoelectrochromic systems

Student Number: 2012-23977

Contents

List of Tables

List of Figures

Chapter 1. Introduction

1.1 Electrochromism

Electrochromism is a phenomenon which involves persistent and reversible change in transmittance or reflectance that is associated with an electrochemically induced oxidation-reduction reaction by simultaneous cation and electron injection/extraction. This color change results from the generation of different visible region electronic absorption band on switching between redox states. It is commonly between a transparent state and colored state, or between two colored state[1]. This phenomenon is termed ‘electrochromism’ in 1961 by Platt., whose discussions were amongst the first published. Later, Byker had discussed the historical development of electrochromism more in detail[2].

The electrochromic devices can be classified into three types: solution type, hybrid type and battery type. Most often, for rechargeable batteries, the electrochromic electrode is separated from the charge balancing counter electrode via a suitable electrolyte[3]. This type has three parts; the working electrode (electrochromic electrode), the electrolyte and the counter electrode (ion storage electrode). Both electrodes are thin films which consist of electrochromic materials, transparent conductor materials and

transparent glass. These thin film electrodes can be fabricated by many methods such as by sputtering, electrodeposition, sol-gel, and so on. Thin film electrodes require insertion/extraction of charge-compensating ions during redox cycling[4]. Electrolyte used in electrochromic devices should be transparent and possess ion-delivery properties. In the case of electrochromic systems, two kinds of electrolyte, liquid or solid, are available. Liquid electrolyte which is dissolved a salt has well known for the least electrochemical interference and greatest stability.

They are usually used in electrochromic devices because liquid electrolyte is the easiest to use and reproducible. In addition, high concentration can aid in maintaining liquid-faction at very low operating temperatures[5].

Fig. 1 shows a basic design of battery-type electrochromic device and a transport of positive ions when an electric field is applied. The color changes occur by movement of small cation such as H^+ or Li^+, through the electrochromic electrode, when a potential of only a few volts is applied.

There are four different types of application in electrochromic devices; smart window, variable reflectance mirror, information display, and variable emittance surface. Fig. 2 shows the four different applications of electrochromic devices. The four schemes of systems and applications in devices are quite different. Smart windows are the most important

application of electrochromism. These windows are used in energy-efficient architecture. Because they adjust the inflow of luminous radiation and solar energy through glazing in buildings, energy used for heating or air conditioning can be minimized. A reflectance mirror is fabricated by replacing one side of the smart window with a specula reflecting metallic reflector. When light reflects off this mirror, electrochromic materials go to the colored state and reduce the light via absorption. This system is applied in rear view mirrors in cars or trucks to temporary blindness by light reflectance. White pigment is contained in electrochromic devices, it shows black/white contrast and off-normal viewing properties. The main benefit of this system is that it has a low energy use during operation and therefore, it is used in information displays such as signs or labels to notice some information. Lastly, degree of surface emittance can be controlled, emission or non-emission, by absorbing and reflecting light, it is concerned about temperature stabilization of satellites[4,5].

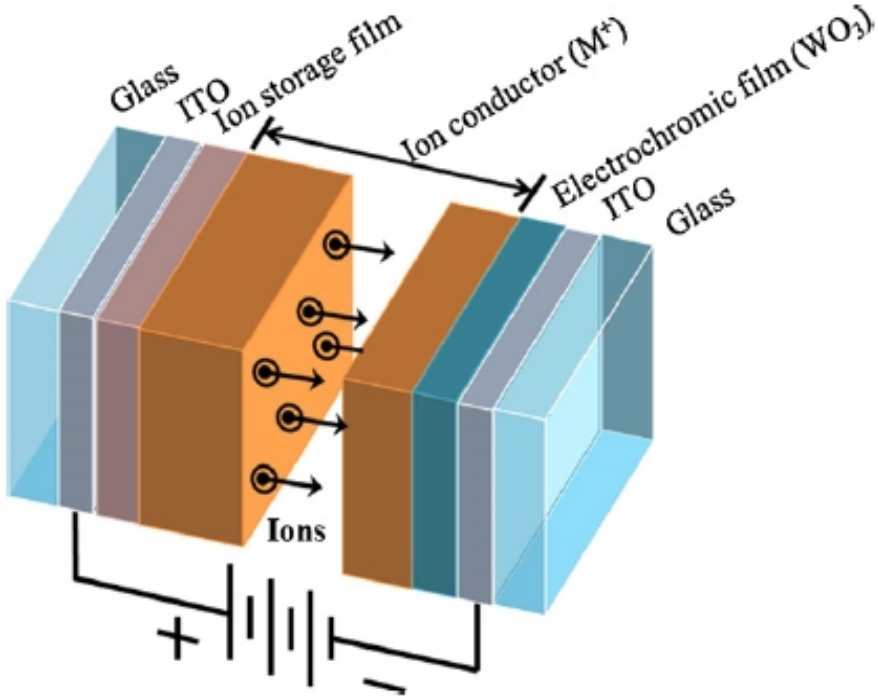

Figure 1. The basic design of battery-type electrochromic device.

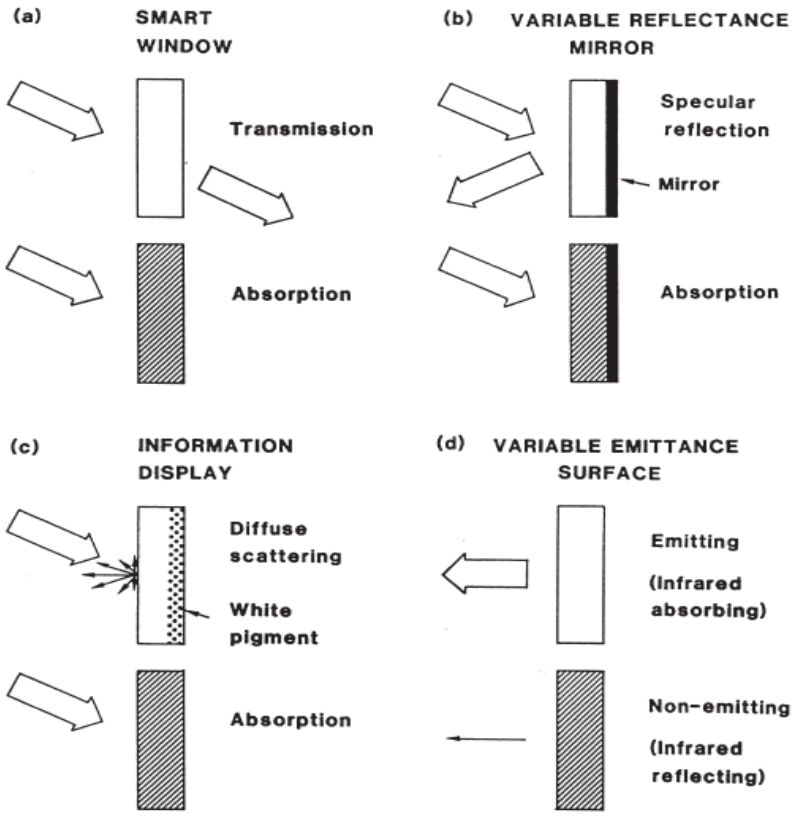

Figure 2. The principle of four different applications of electrochromic devices (Arrows indicate incoming and outgoing electromagnetic radiation intensity).

1.2 Types of electrochromic materials

Materials have shown an electrochromism largely classify organic and inorganic materials. Conductive polymer materials mainly produce organic systems. Organic materials are enticing due to various color options, high contrast, and fast response time.

On the other hand, inorganic systems often employ transition metal oxides (TMOs). Table 1 illustrates the metal oxides known to produce cathodic and anodic electrochromic oxides.

Depending on its oxidation state, Ni oxide can exist in a colorless reduced form or a dark brown oxidized form. Because Ni oxide has a large contrast ratio between colored and bleached state and good optical balance with WO_3, they are a good candidate for a counter electrode material of WO_3[6].

In addition, the layered structure of V pentoxide films makes them well suited as hosts for ion intercalation/deintercalation, so V pentoxide are commonly used as an ion storage layer. They have the visible color change from a yellow pale blue to brown/yellow[7].

Ir oxide, which has a visible color change from colorless to dark blue, is also widely researched as a counter material of WO_3. The electrochromic reaction was different from aqueous electrolyte and small alkali-ion electrolyte. Although Ir oxide has good electrochromic properties, high price

of this material was the hindrance for commercialization[8].

Among the cathodic colored electrochromic TMOs materials reported thus far, WO_3 has remained the most widely used material due to its higher coloration efficiency, better cycle stability compared with other TMOs and high contrast ratio between transparent and deep-blue. High color efficiency can render an obvious optical modulation by a small change of the inserted cations, thus promising long-term stability of the host matrix. It is comprised of a corner-sharing WO_6 octahedral which is known as the defect perovskite structure. Ions such as protons or other cations can be intercalated or deintercalated during the reversible electrochromic reaction through the space region between the octahedral[9].

Metal Oxide	Reaction	Colour Change
Cobalt Oxide	$3CoO + 2OH \rightarrow Co_3O_4 + H_2O + 2e^-$	green → brown
Indium Tin Oxide	$In_2O_3 + 2x(Li^+ + e^-) \rightarrow Li_{2x}In^{III}_{(1-x)}In^{I}_{x}O_3$	colourless → pale blue
Iridium Oxide	$Ir(OH)_3 \rightarrow IrO_2 \bullet H_2O + H^+ + e^-$	colourless → blue/grey
Molybdenum Trioxide	$MoO_3 + x(Li^+ + e^-) \rightarrow Li_xMo^{VI}_{(1-x)}Mo^{V}_{x}O_3$	colourless → blue
Nickel Oxide	$NiO_xH_y \rightarrow [Ni^{II}_{(1-z)}Ni^{III}_{z}]O_xH_{(y-z)} + zH^+ + ze^-$	colourless → brown/black
Tungsten Trioxide	$WO_3 + x(Li^+ + e^-) \rightarrow Li_xW^{VI}_{(1-x)}W^{V}_{x}O_3$	very pale blue → blue
Vanadium Pentoxide	$Li_xV_2O_5 \rightarrow V_2O_5 + x(Li^+ + e^-)$	very pale blue → (brown/yellow)
Cerium Oxide	$CeO_2 + x(Li^+ + e^-) \rightarrow Li_xCeO_2$	yellow → very pale
Manganese Oxide	$MnO_2 + ze^- + zH^+ \rightarrow MnO_{(2-z)}(OH)$	yellow → brown
Niobium Pentoxide	$Nb_2O_5 + x(Li^+ + e^-) \rightarrow Li_xNb_2O_5$	colourless → pale blue
Ruthenium Dioxide	$RuO_2 \bullet 2H_2O + H_2O + e^- \rightarrow \frac{1}{2}(Ru_2O_3 \bullet 5H_2O) + OH^-$	(blue/brown) → black

Table 1. Some examples of electrochromic metal oxides.

1.3 Photoelectrochromic devices

Photoelectrochromic devices are a combination of dye-sensitized solar cells and electrochromic layers. In contrast to electrochromic devices, no external voltage source is necessary for coloring. Furthermore, in contrast to photochromic devices, the system is externally switchable. The transmittance can be decreased under illumination and can be increased again in the dark.

It was first reported by Bechinger *et al*. in 1996 and they demonstrated a change in transmittance from 70 to 53% in about 1 min. The bleaching time was about 4 min. This low transmittance change could be explained by short circuit current[10]. The design of the photoelectrochromic device is shown in Fig. 3. It consists of a dye-covered nanocrystalline TiO_2 layer on a TCO coated glass substrate on the one side and a WO_3 layer on a TCO-coated substrate on the opposite side. The pores of the WO_3 and TiO_2 layers and the space between them are filled with the electrolyte (e.g. LiI in propylene carbonate).

After 5 years later, new photoelectrochromic device with a modified layer configuration was developed by A. Hauch *et al*(Fig. 4). In new photo-electrochromic device, the photoactive layer (dye-sensitized TiO_2) is situated on the electrochromic WO_3 layer. The opposing electrode is a platinized

TCO-coated glass. This device has the advantage that the bleaching process can be accelerated by a catalyst independently of the coloration process compared to the conventional photoelectrochromic device. The electrolyte contains Li^+ and a redox couple (I^- and I^{3-}) in an organic solvent (e.g. propylene carbonate). When under open circuit conditions and illuminated, photoelectrons generated at the anode move to the WO_3 electrode via an external circuit, which drives Li ions in the electrolyte to intercalate into WO_3 in order to keep the charge balanced. Consequently Li_xWO_3 is formed, which possesses a color different from the starting material. The colored cell is bleached in the dark at short circuit, but the bleaching rate is rather slow. In the dark, a voltage equal to the photovoltage, but of opposite polarity, appears across the device and drives the electrons back to the TiO_2 and from there into the electrolyte. The WO_3 is bleached. The bleaching process is limited by the electron transfer from TiO_2 into the electrolyte, which is an unwanted loss reaction in the dye-sensitized solar cell. This means that if the bleaching is fast, the coloring is weak and slow, because coloring and bleaching are competing processes[11,12].

Applications of these devices include, but are not limited to, switchable sunroofs in cars or smart windows in buildings.

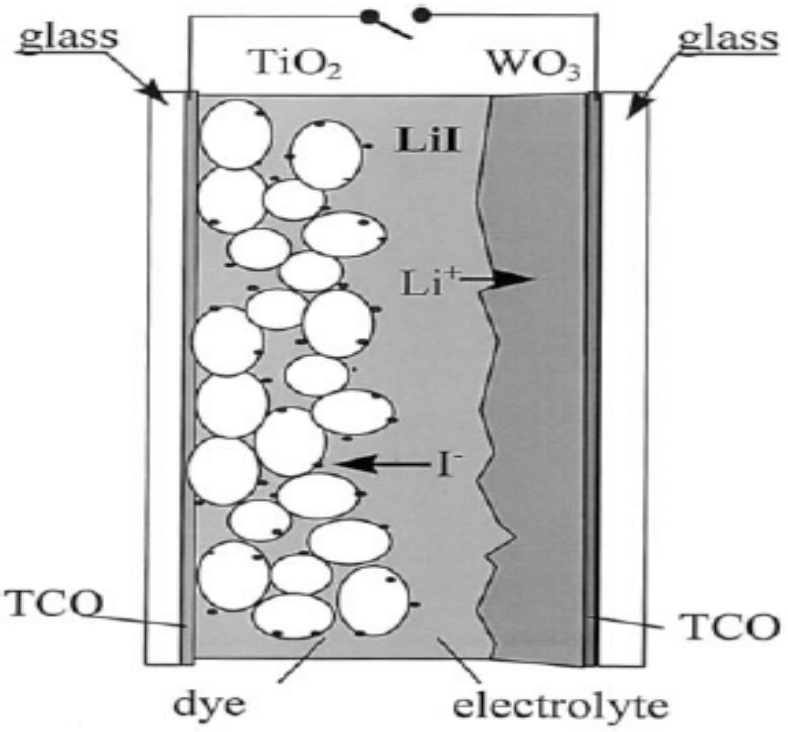

Figure 3. Photoelectrochromic device with TiO_2 and WO_3 on separate surfaces.

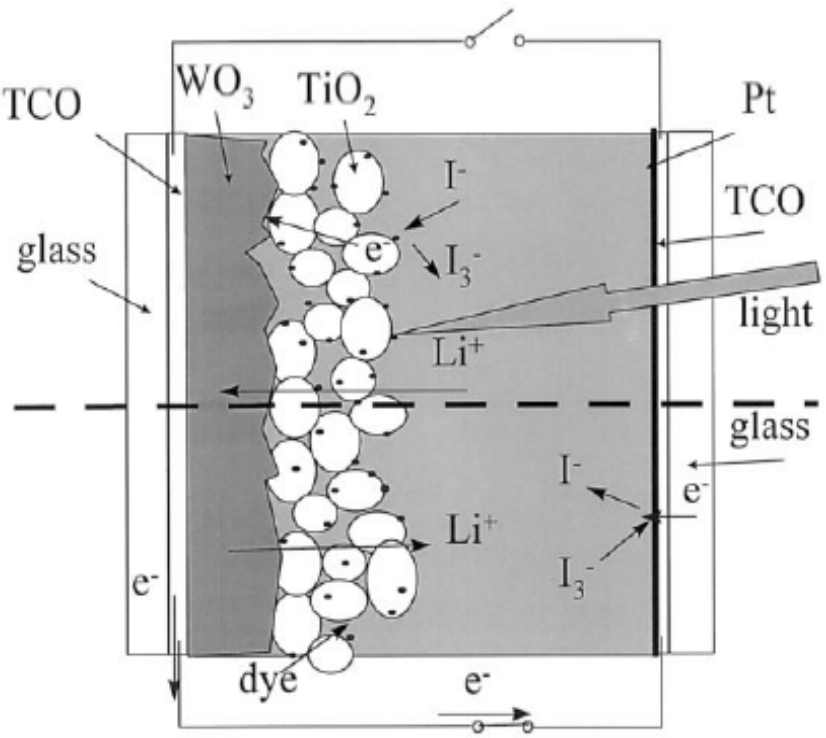

Figure 4. The design of the new photoelectrochromic device.

1.4 Overview of this study

Out of many electrochromic materials, this study has focused on WO_3 because WO_3 electrochromic films have been fabricated by many research groups for not only enhancing electrochromic performance but employing photoelectro-chromic systems due to the suitable band position with TiO_2 in these systems.

In addition, it has been reported that the optical properties of WO_3 films colored upon cations insertion rely critically upon the morphology and crystallinity of WO_3[13,14].

In this study, WO_3 thin films were prepared by using a sol-gel method in a precursor solution dissolved in ethanol. This solution was deposited on the FTO glass under room temperature by repeated dip coating for film thickness control and deposited film was annealed at 200℃ for amorphous phase. The WO_3 thin films had a μm or nm-scale thickness and the optimum thickness exhibiting the best electrochromic performance was decided for employing to photoelectrochromic systems. WO_3 thin films exhibited good electrochromic performance in a lithium-based electrolyte, such as enhanced charge capacity, increased optical transmittance changes in a three-electrode electrochemical test.

After that, this film was applied to the two-type of photoelectrochromic

systems with two parameters, the thickness and annealing temperature of the WO_3 thin film. This work was for observing the photoelectrochromic optical transmittance kinetic tendencies with illumination time goes on and the comparison it with that of crystalline phase and film thickness dependent electrochromic properties of WO_3 thin films prepared by sol-gel dip-coating method.

Chapter 2. Theory

2.1 The theory of sol-gel method

Electrochromic films are deposited as a thin film. The major methods of deposition classified into physical, chemical, and electrochemical ones and further subdivided into varieties[2]. Among many deposition methods, sol-gel process is a chemical method widely used for synthesizing transition metal oxide coatings. The fundamental of sol-gel was introduced by C. J. Brinker in 1991[15]. Originally, this method was used to prepare pure ceramics precursors and inorganic glasses at relatively low temperatures. “Sol” is short for any suspension, colloids or inorganic mono-molecules that are dispersed in solution, and “gel” is designated that the solution has lost liquid like properties by network structure of molecules. The sol-gel method is mainly divided into the alkoxide method and colloid method. Inorganic materials often employ the alkoxide sol-gel method which is generally divided into two step: hydrolysis and condensation[16].

Hydrolysis:

$$M\text{-}OR + H_2O \rightarrow M\text{-}OH + R\text{-}OH$$

Condensation:

Alcohol condensation (Alcoxolation)

$$M\text{-}OR + HO\text{-}M \rightarrow M\text{-}O\text{-}M + R\text{-}OH$$

Water condensation (Oxolation)

$$M\text{-}OH + HO\text{-}M \rightarrow M\text{-}O\text{-}M + H_2O$$

Where $M(OR)_n$, M represents a network-forming element such as Si, Ti, Zr, Al, B, etc., R is typically an alkyl group (C_xH_{2x+1}) and $M(OR)_n$ represents metal or semimetal alkoxide precursors. During sol-gel reaction, many parameters such as pH, water content, properties and concentration of catalyst (acid or base), temperature, and drying condition can change the reactivity scheme and the properties of final product. For example, nucleophilic reaction and faster condensation occur, and highly branched clusters are formed under base catalyst. While, in condition of acid catalyst, electrophilic reaction and faster hydrolysis occur, and primarily linear or randomly branched structure is formed. These parameters also can affect pore size, pore volume, and specific surface area[16].

Synthesis via this method has many benefits. Since it employs a low temperature process, thermal degradation can be minimized and high purity and stoichiometry can be easily achieved. Therefore, high purity nano-crystalline materials or amorphous oxide materials can be easily produced. By

appropriate chemical modification of the precursors, colloid particle size, pore size, porosity, pore wall chemistry of the final material, and microstructure of the films can be easily controlled.

Liquid precursors are usually used in sol-gel method, it is possible to make various shapes such as fibers, monoliths, and thin films at low cost compared to other thin film processing methods. However, the methods need a careful aging and drying process, change volume on densification and shrinkage or cracking on drying, and take a long time for completing the whole process[16].

2.2 The theory of dip-coating

There are many methods for coating of films related to sol-gel method. The most popular method is the dip-coating method because it is a fast and efficient method. The process of dip-coating method is divided into five steps; immersion, start-up, deposition, drainage, evaporation. All of these steps are described as follows and Fig. 5[15] shows these by sequential stages of structure development.

1. Immersion: The substrate is immersed in the solution of the coating material at a constant speed.

2. Start-up: The substrate has remained inside the solution for a while and is

starting to be pulled up.

3. Deposition: The thin layer deposits itself on the substrate while it is pulled up. The withdrawing is carried out at a constant speed to avoid any jitters. The speed determines the thickness of the coating (faster withdrawal gives thicker coating material).

4. Drainage: Excess liquid will drain from the surface.

5. Evaporation: The solvent evaporates from the liquid, forming the thin layer. For volatile solvents, such as alcohols, evaporation starts already during the deposition & drainage steps.

Film thickness is controlled by coating viscosity (η) and rate of withdrawal (U) from the container. The faster a substrate is withdrawn from the container of the sol, the thicker the coating material is applied to the substrate. The lower viscosity solution is used in coating, the thinner films would be obtained. In addition, rate of withdrawal and solution viscosity are not large enough in dip-coating method, the ratio between liquid-solid surface tension (γ_{LV}) also affects the film thickness. Therefore, film thickness (h) is calculated by the landau-levich equation.

$$h = \frac{0.94(\eta U)^{2/3}}{(\gamma_{LV})^{1/6}(\rho g)^{1/2}}$$

Where g represents the acceleration of gravity and ρ represents density of solution[17].

Although dip-coating is popular, it is not without its drawbacks. These include, but are not limited to lighter parts tending to float and fall from the conveyor and film thickness varying from top to bottom ("wedge effect").

Therefore, to obtain excellent thin films via the dip-coating method, these factors must be considered and accounted for. For the coating material to apply itself uniformly to the substrate during dwelling times, the substrate must be fully immersed and remain motionless while in the sol. Withdrawal of the substrate must be done at a constant speed to avoid any judders.

Up until now, many variations of the dip-coating technique have been reported. For example, the comparative study of spin and dip coated nanostructured thin films revealed a superior performance for the cycled dip coated film in terms of higher transmission modulation and coloration efficiency in solar and photonic regions, faster switching speed, higher electrochemical activity as well as charge storage capacity[20]. Tailoring for large-scale patterning of nanowires[21] and a rapid, continuous, utilization of mesostructures in thin-film form by dip coating technique was also previously

reported[22].

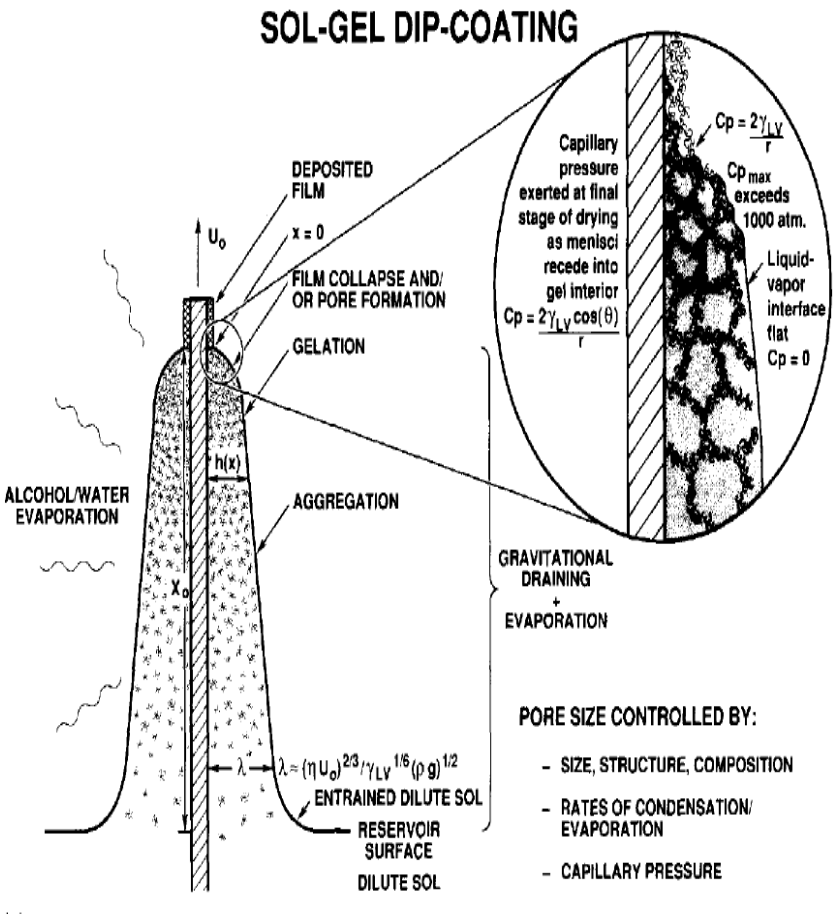

Figure 5. Schematic diagrams of the steady state dip-coating process.

2.3 The values for electrochromic materials

2.3.1 Coloration efficiency (CE)

Visible color change is an important characterization of electrochromic system. Therefore, to know how much the color change is essentially required in electrochromic system. Contrast ratio (CR) is known below.

$$CR = \frac{R_0}{R_x}$$

Where R_x is the intensity of light diffusely reflected through the colored state, and R_o is the intensity of light diffusely reflected from bleached state. If contrast ratio has large value, it means that difference of transmittance at colored/bleached state in electrochromic device is quite comparable[2].

The optical absorption is also shown by the Beer-Lambert law. It represents that the absorbance expressed as log of the ratio of the intensities is proportionally related to the concentration and optical path length through the sample. In transmittance mode, the optical absorption in electrochromic film has similar expression of the Beer-Lambert law. This expression, related to the injected charge per unit area Q, is shown below since Q is proportional to the number of color centers.

Beer-Lambert law: $A = \log \frac{T_b}{T_c} = \varepsilon cl$

The optical absorption in electrochromic film: $A = \log \frac{T_b}{T_c} = \eta Q$

Where A is the absorbance, T_c is the intensity of transmitted light in the colored state, T_b is the intensity of transmitted light in the bleached state, and η is the coloration efficiency (CE) of the film[2].

Therefore, the coloration efficiency (CE) is related to an optical change (△OD) and charge density (Q) per unit area.

$$\eta = \frac{\Delta OD(\lambda)}{Q}[cm^2 / C]$$

$$\Delta OD(\lambda) = \log \frac{T_b}{T_c}$$

It shows the ratio of the intensities in optical absorption when a charge is injected in the film. If CE is large, it represents that change in optical absorption is large and required charge is small. This may be a good electrochromism. In general, organic electrochromes exhibit a greater η than inorganic species because the molar absorptivity of the former are usually higher than later[2].

2.3.2 Response time

The time required to coloration from its bleached state is called response time.

For most electrical devices, response times are represented by the order of a few seconds. For electrochromic devices, in general, response time is slower than for either liquid crystal display (LCD) or cathode ray tube (CRT).

Electrical conductivity of conducting layer, the ion diffusivity of electrolyte and ion diffusivity or electrical conductivity of electrochromic materials, is an important factor in the response time of an electrochromic device. For example, response time of organic electrochromic materials generally is much faster than that of inorganic electrochromic materials and the ion diffusivity of solid electrolyte is slower than that of liquid electrolyte.

There is no consistency in the criteria employer for determining response time. It may be the time necessary for some fraction of the color to form, such as is indicated by particular increment of optical density, or the time for all or part of the charge to be injected. Because of these inconsistencies in reporting response time, any comparison of response time would be limited value[2]. In this study, the time for a percentage of 90 in optical change, from colored state to bleached state, is called response time.

2.3.3 Cycle life

When an electrochromic device is continually cycled between its colored and bleached states, device failure will eventually occur resulting from physical change in solid phases or from chemical side reactions. The cycle life is a measure of its stability, being the number of the cycles possible before such failure. A major aim of device fabrication is obviously to maximize the cycle life. In some tests of electrochromic devices, extensive cycling, cited as evidence of robustness, involves cycles of duration considerably shorter than the response time. Such tests are clearly of extremely limited value. The cycle life is a complicated function of the coloration required in the cycle: the cycle life generally decreases if wide changes in composition are required, that is, if the quantity of charge injected or removed is large. Some authors attempt to address the variation in severity of the test inherent here by denoting a cycle life as involving ‘deep’ or ‘shallow’ cycle, cycles of duration markedly less than τ for total color switching indicating ‘shallow’ cycles. Cycle lives, being thus generally ill defined or at best only roughly illustrative, are therefore not tabulated[2].

Chapter 3. Experimental

3.1 Preparation of WO_3 thin film

Based on a previous reports[18, 19], WO_3 electrochromic thin film was prepared by sol-gel method. 0.1 M tungsten metal monocrystalline powder (Aldrich, 99.9$^+$%) and hydrogen peroxide (Junsei, 30%) were used as the precursor and solvent, respectively. This solution was poached at 100 ℃ about 1 hour and kept for 2 hours at room temperature for cooling down. And then, diluted by adding the EtOH with 1:4 volume ratio followed stirring for 2 days at room temperature.

Finally, orange-colored viscous solution was obtained. Compared with before poaching process, this solution had a clear orange color and heavier viscosity.

Thin films were deposited by using dip-coater (Kwanghak Mechanical Eng. Co. Ltd., Korea). The substrates for thin film deposition were fluorine-doped tin oxide glass (FTO glass; Pilkington glass Co. Ltd.). These substrates were dipped into the coating solution for 5 minute and withdrawn at 6 cm/min speed. During thin film deposition, we maintain a room temperature and low humidity to get uniform WO_3 thin film having fine surface. By repeating the dip-coating process, film thickness could be controlled. After that, the coated

thin films were dried in 80 ℃ oven about 40 minute.

And then, dried films were treated annealing at 200 ℃ for 2 hours by applying two step processes. Heat was given by the increasing rate of 2 ℃/min at first step. When temperature reached at 100 ℃, this temperature was kept for 30 minute to evaporate solvent. After that, heat was given by the increasing rate of 2.5 ℃/min to reach 200 ℃. Lastly, thin film was annealed at 200 ℃ for 2 hours and annealing process was needed to transfer $W(OH)_6$ to WO_3. The annealing temperature affected optical modulation, charge density and crystalline phase of thin film, so we optimized temperature up to 200 ℃ to obtain best coloration efficiency and maintain the amorphous phase of thin film.

In this overall process, we could obtain about 350-1100 nm WO_3 thin film by repeated dipping of FTO substrates. Fig. 6 was shown the overall flow chart of fabrication of amorphous WO_3 thin film.

3.2 Preparation of photoelectrochromic cell

Transparent TiO_2 layers of 3-μm thickness were deposited either onto the WO_3 film or a FTO glass by doctor-blading technique using a commercial TiO_2 paste (DSL 18NR-T, Dyesol) followed by sintering at 500 ℃ for 30 mins.

For the photoelectrochromic cells employing TiO_2 deposited WO_3 electrode, Pt-FTO electrode fabricated by thermal decomposition (spin coating the FTO glass with 50 mM H_2PtCl_6 dissolved isopropanol solution and thermal treatment at 450 ℃ for 20 mins) was used as a counter electrode. For the cells based on TiO_2 coated FTO, WO_3 film prepared by the same method described in chapter 3.1 was used as the electrochromic counter electrode. The only differences were the temperatures for the thermal annealing, which were 200 ℃ and 500 ℃. 50 μm thick thermoplastic sealants (Surlyn, Dupont) were used for the cell assembly, and 0.5 M LiI and 0.005 M I_2 in propylene carbonate (PC) was used as the electrolyte. The active area of the samples for optical property test was 1.5 x 1.5 cm^2.

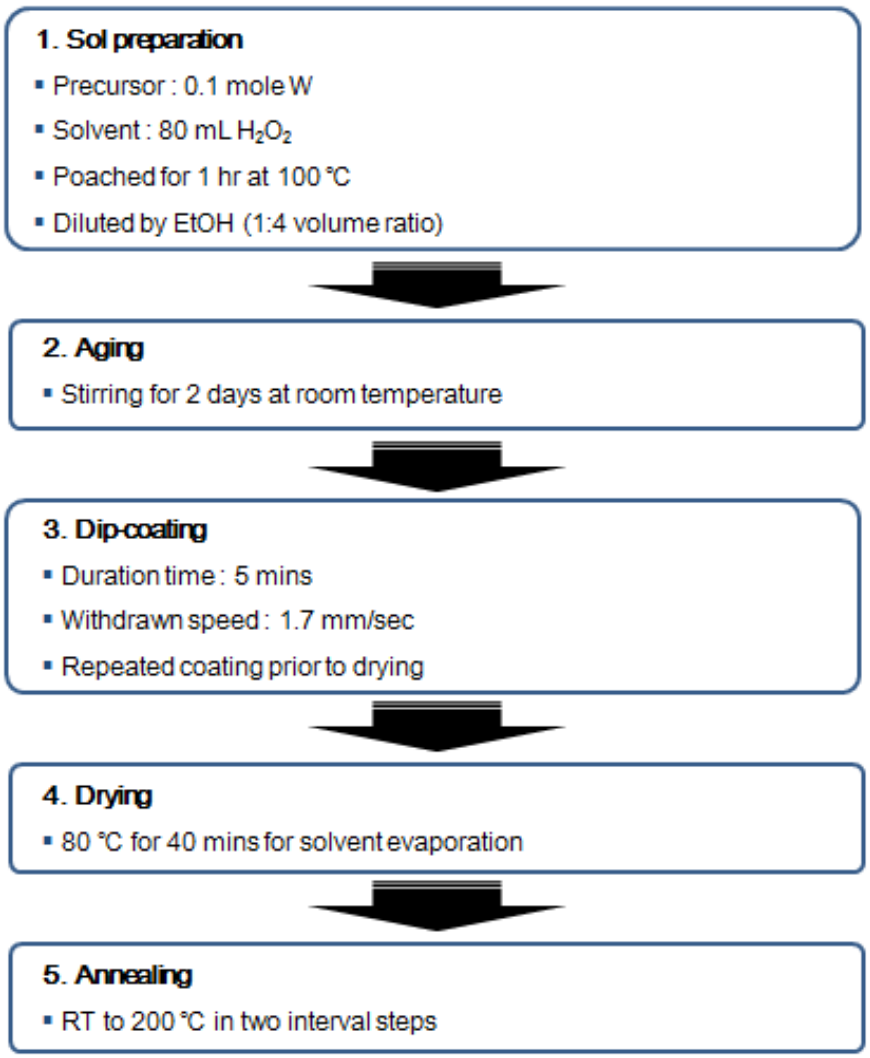

Figure 6. The fabrication processes of amorphous WO_3 thin film.

3.3 Characterization

3.3.1 Material analysis

The characteristics of WO_3 thin films were examined following analytical techniques. The phase and structure of thin films were investigated by XRD (X-ray diffraction, Rigaku D-MAX2500-PC) with a Cu-Kα radiation (λ=1.54178 Å).

The morphology and thickness of the WO_3 films were characterized by Field emission scanning electron microscopy (FE-SEM, JEOL JSM 6700F).

3.3.2 Electrochemical and optical properties

The electrochemical tests were measured by a potentiostat/galvanostat (AutoLab PGSTAT30). All electrochemical tests were conducted in lithium-based electrolyte. The electrochemical cell for half-cell test was composed by three-electrode; working electrode (WE), counter electrode (CE) and reference electrode (RE). Pt wire was used as a counter electrode and Ag/AgCl (sat. KCl) was used as a reference electrode. A solution of 1 M $LiClO_4$ (Aldrich, 95^+%) in propylene carbonate anhydrous (Aldrich, 99.7%) was used as a lithium-based electrolyte for electrochemical tests.

In this study, cyclic voltammetry (CV) and continuous potential cycling

with chronocoulometry (CC) method were used to measure the electrochemical properties. CV was conducted in voltage range between -1.2 and 1.2 V and 10 cycles of continuous potential cycling with CC was performed in the range of -1 and 1 V with a duration time of 30 seconds. In this tests, the change of transmittance in colored/bleached state could be shown by an in-situ optical transmittance system using He-Ne laser (λ=633 nm) and potentiostat. We calculated the transmittance changes by using standard condition in fully bleached state as a 100% transmittance at room temperature. These test system was shown in Fig. 7. The 1000 cycles of the change of transmittance with continuous potential cycling was also performed in the same voltage range for observing the long-term stability of WO_3 thin film.

3.3.3 Photoelectrochromic properties

The electrochemical tests were measured by a UV-vis spectrometer (Jasco V-670) for observing the transmittance changes in the visible, adjacent near-infrared (NIR) and IR regions of two types of the photoelectrochromic systems with illuminated time goes on.

In this test, we could compare the transmittance switching kinetics with thickness and crystalline phase of WO_3 in layered and separate structure of

photoelectrochromic cells, and also compare it with crystalline phase and film thickness dependent electrochromic properties of WO_3 thin films prepared by sol-gel dip-coating method.

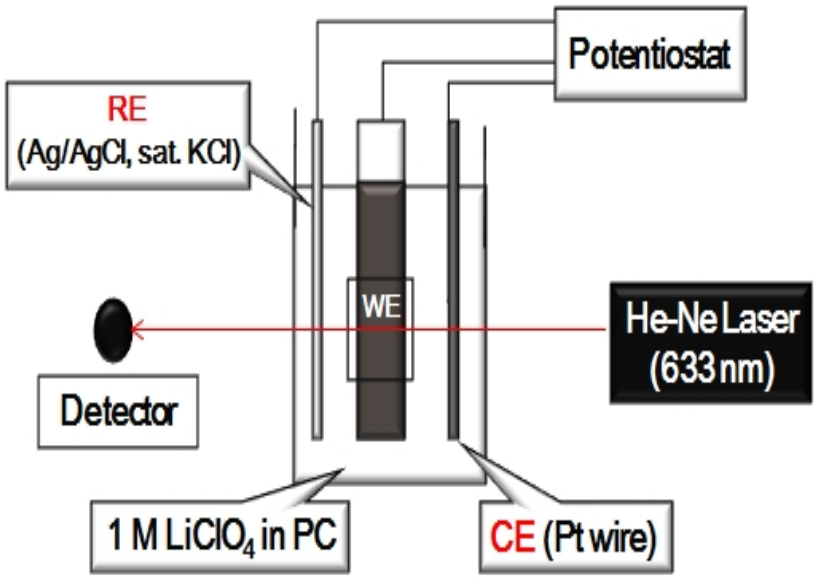

Figure 7. Experimental scheme of electrochemical and optical test.

Chapter 4. Results and discussions

4.1 Electrochromic characterization

4.1.1 Material analysis

To compare with before and after annealing process at 200 ℃ of WO_3, XRD measurement was taken. Fig. 8 was shown the XRD patterns of the three times coated WO_3 thin films. WO_3 thin film after heat annealing process was (a) and after drying process was (b). The bare FTO glass substrate and monoclinic WO_3 peak position were referenced at the bottom of the fig. 8 as a bar shapes for easy comparisons.

As shown in Fig. 8(a) and (b), no peaks from the precursor were observed in this film both before and after heat annealing process and only substrate peaks appeared. These results prove that heat annealing process at 200 ℃ did not affect the amorphous phase of WO_3 although dip-coating process was repeated several times. So, it notes that amorphous phase WO_3 thin films were successfully deposited on the FTO glass substrate.

The morphology, film adhesion with substrate and thickness of once coated WO_3 thin films were shown in SEM image of fig. 9. In fig. 9(b), it was shown that after heat annealing process, WO_3 thin film had a good adhesion

with substrate and fine surface compared with before heat annealing process in fig. 9(a). The surface morphology of WO_3 thin film by repeated dip-coating was shown in Fig. 10(a-e). It was believed that there is no difference of surface morphology from once coated to five-times coated film.

In addition, the thickness of these films measured by each cross-section FE-SEM image was shown in Fig. 11(a-e). Compared with a once coated film (1.1 μm), three-times coated film was thinner (460 nm) and four-times coated film was the thinnest among the five different samples. Thickness range of each sample was shown in fig. 11(f) for indicating the few differences of thickness value with position in same sample.

Approximately, the thickness of deposited thin film was observed to inversely proportional to the repeating number of dip-coating process.

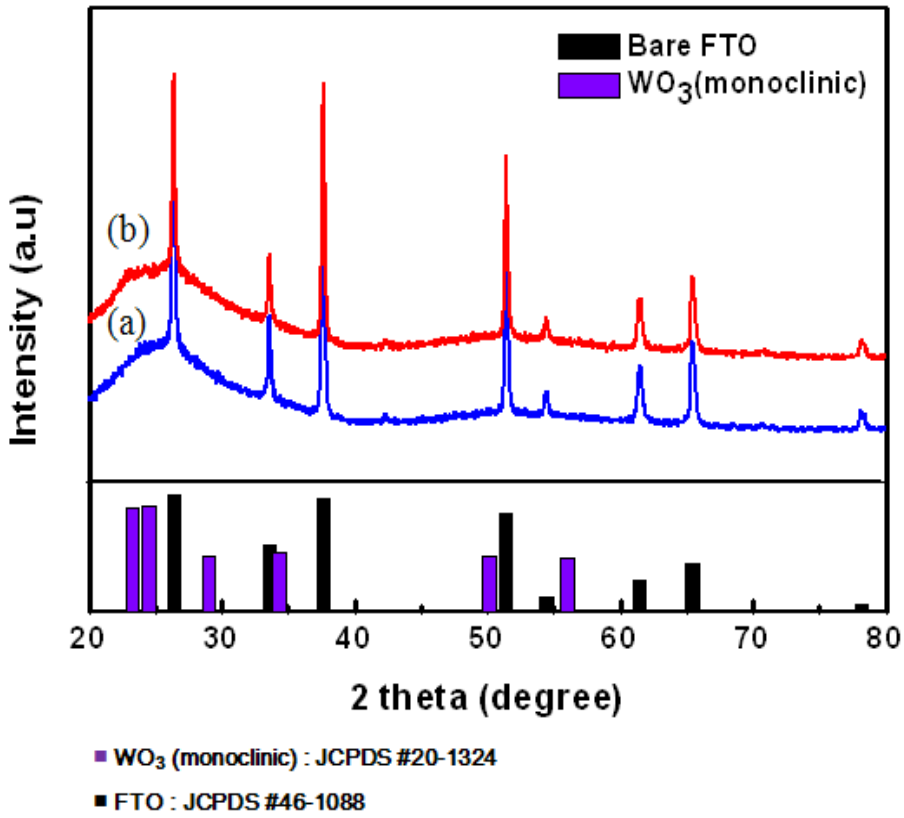

Figure 8. XRD patterns of three-times coated WO_3 thin film; (a) annealed at 200 ℃ and (b) dried at 80 ℃.

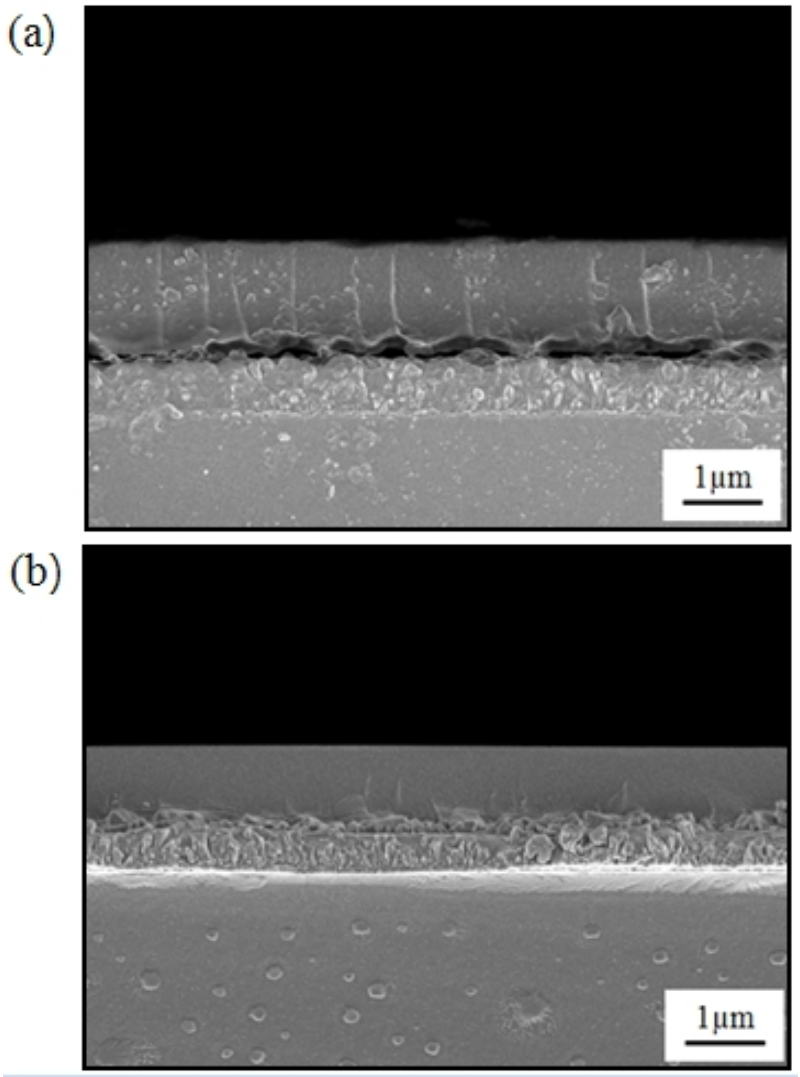

Figure 9. Cross-sectional image of once coated WO_3 thin film; (a) dried at 80 ℃ and (b) annealed at 200 ℃.

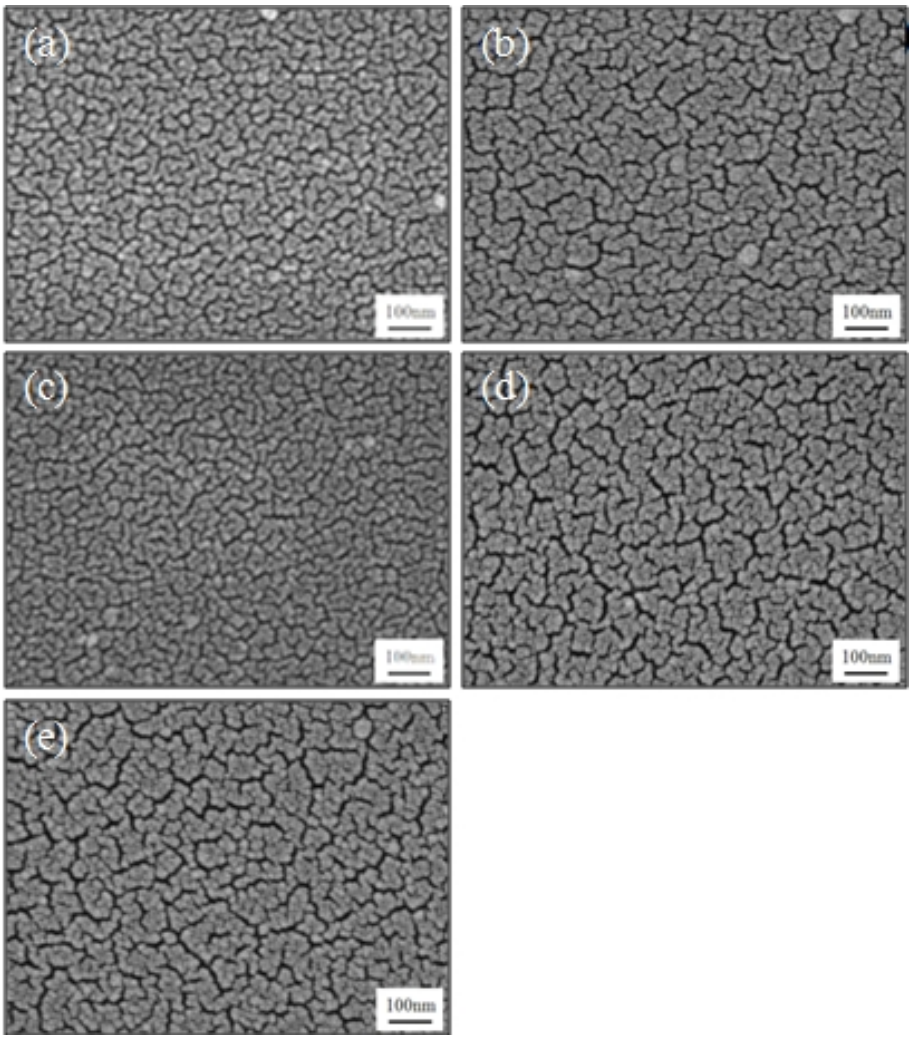

Figure 10. FE-SEM images of WO_3 thin film; (a) once, (b) twice, (c) three-times, (d) four-times, and (e) five-times coated film.

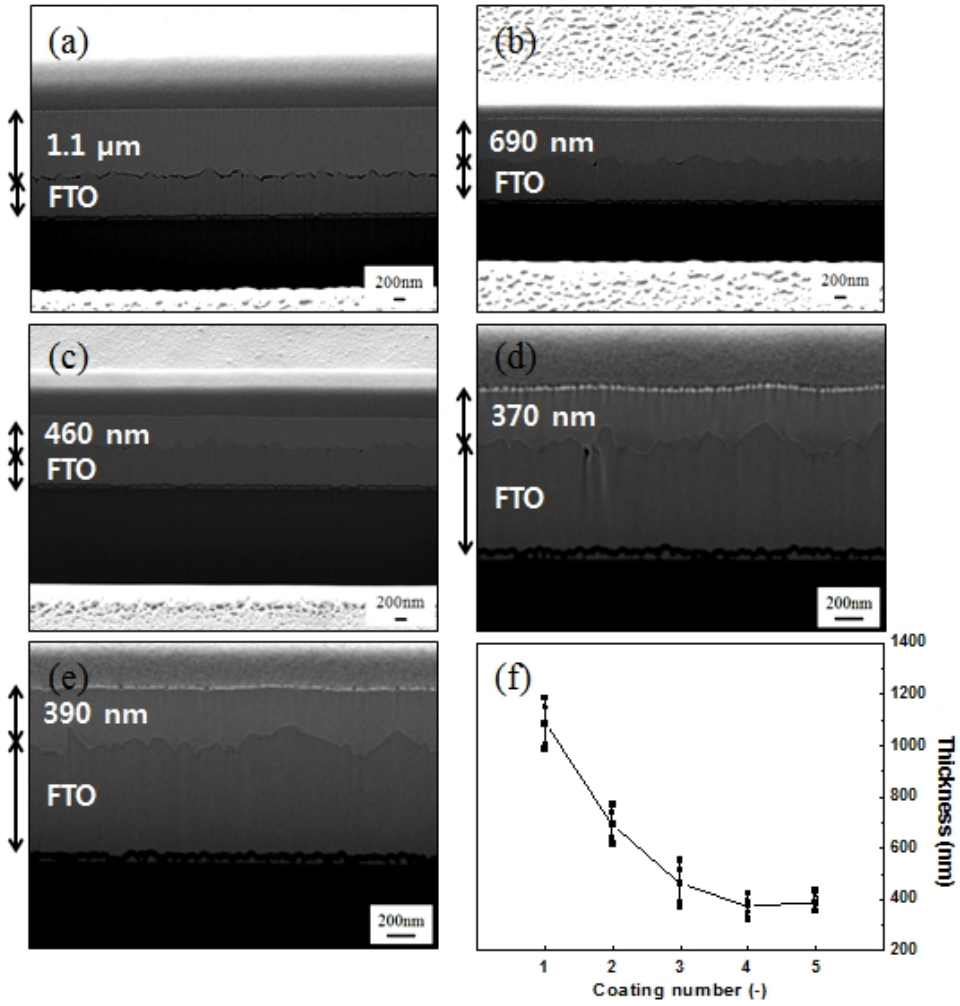

Figure 11. The thickness of WO_3 thin film; (a) once, (b) twice, (c) three-times, (d) four-times, (e) five-times coated film, and (f) film thickness with error bars.

4.1.2 Electrochemical and optical properties

Fig. 12(a) showed the cyclic voltammogram of the WO_3 thin film with repeated coating number. We measured 10^{th} cycle at a scan rate of 20 mV/s carried out in solution of 1 M $LiClO_4$ in propylene carbonate (PC) vs. Ag/AgCl (sat. KCl) reference electrode.

The shapes of the CV curves were similar for all samples. The three-times coated film, however, showed slightly larger current densities (higher exchanged charge densities) compared to others, which reflects the fact that lithium ions insertion/extraction into the host lattice was facilitated at a given applied potential[23]. Furthermore, the onset potential of the cathodic current for the three-times coated film was slightly shifted in the positive direction compared to the others. That is, insertion could be achieved at a considerably lower applied voltage. So, I think the electrochromic properties of charge acceptance might be enhanced compared with others.

So, we measured charge density during cyclic test with fixed voltage range. Fig. 12(b) showed the charge density with the repeated coating number. The three-times coated film had the largest charge density of 28.53 mC/cm^2. It was so remarkable value compared to that of other electrochromic film deposition techniques and it might be attributed two factors; the thickness of film and adhesion of thin film with substrate. As we explained in material

analysis section, as coating number increased, thinner film was obtained.

Thinner film had advantage of fast cation movement into the host lattice with electrons although total charge capacity of film was small compared with thicker film. This indicated that even a higher lithium ion movement was provided with electrons due to the short pathway of ions.

To quantitatively compare the optical properties of the electrochromic thin films, transmittance measurements were performed by using the *in-situ* transmittance measurement technique.

Fig. 13(a) showed *in-situ* transmittance curves obtained during the continuous potential cycling applied between -1.0 and 1.0 V. All transmittance data were measured in He-Ne laser (633 nm) and normalized by the transmittance in fully bleached state in air at room temperature.

Consequently, three-times coated film exhibited the largest optical transmittance changes (about 69.7% at bleached state and 4.7% at colored state). Long-term stability of three-times coated film was also quite good as shown in fig. 13(b). This test was measured in same condition of 1,000 cycles with continuous potential cycling.

The coloration efficiency (CE) was expressed as the ratio between the contrast in the bleached state (T_b) and the colored state (T_c) with charge capacity (Q); $CE = \log(T_b/T_c)/Q$. As shown in table 2, the coloration

efficiency of three-times coated film was 1.3 times higher that of once coated film, which was similar value compared to five-times coated film, but slightly poor than four-times. But in terms of charge capacity and optical transmittance changes, three-times coated film exhibited the quite remarkable electrochromic properties among samples.

In addition, as shown in fig. 14(a) and (b), three-times coated film exhibited higher charge capacity and optical modulations both during 1^{st} and 10^{th} cycle than others. So, we decided the optimum thickness of thin film exhibiting best electrochromic performance and employed it to the two types of photoelectrochromic systems in next chapter.

Fig. 15 showed charge capacity and optical modulations of WO_3 thin film heat annealed at 500 ℃ with same measurement condition of heat annealed at 200 ℃. From the comparison of fig. 12(b) and fig. 15(a), crystallized WO_3 thin film exhibited extremely poor charge density compared to amorphous phase both once coated and three-times coated film.

It is believed that charge extraction reaction occurred slowly in crystallized WO_3, so few amount of charge inserted in film were not extracted completely.

When comparing optical property of three-times coated film that had amorphous and crystalline WO_3 from fig. 13(a) and fig. 15(b), crystalline

WO_3 thin film annealed at 500 ℃ also exhibited quite poor optical changes about one-third compared to amorphous film (about 48.61% in bleached state and 24.76% in colored state at first cycle).

In addition, in the case of crystallized WO_3 film, quite severe optical degradation occurred during continuous potential cycling even just after 10 cycling. When compared first with 10^{th} cycle, three-times coated film (16.4%) exhibited about two times higher degradation values than that of once coated film (8.1%).

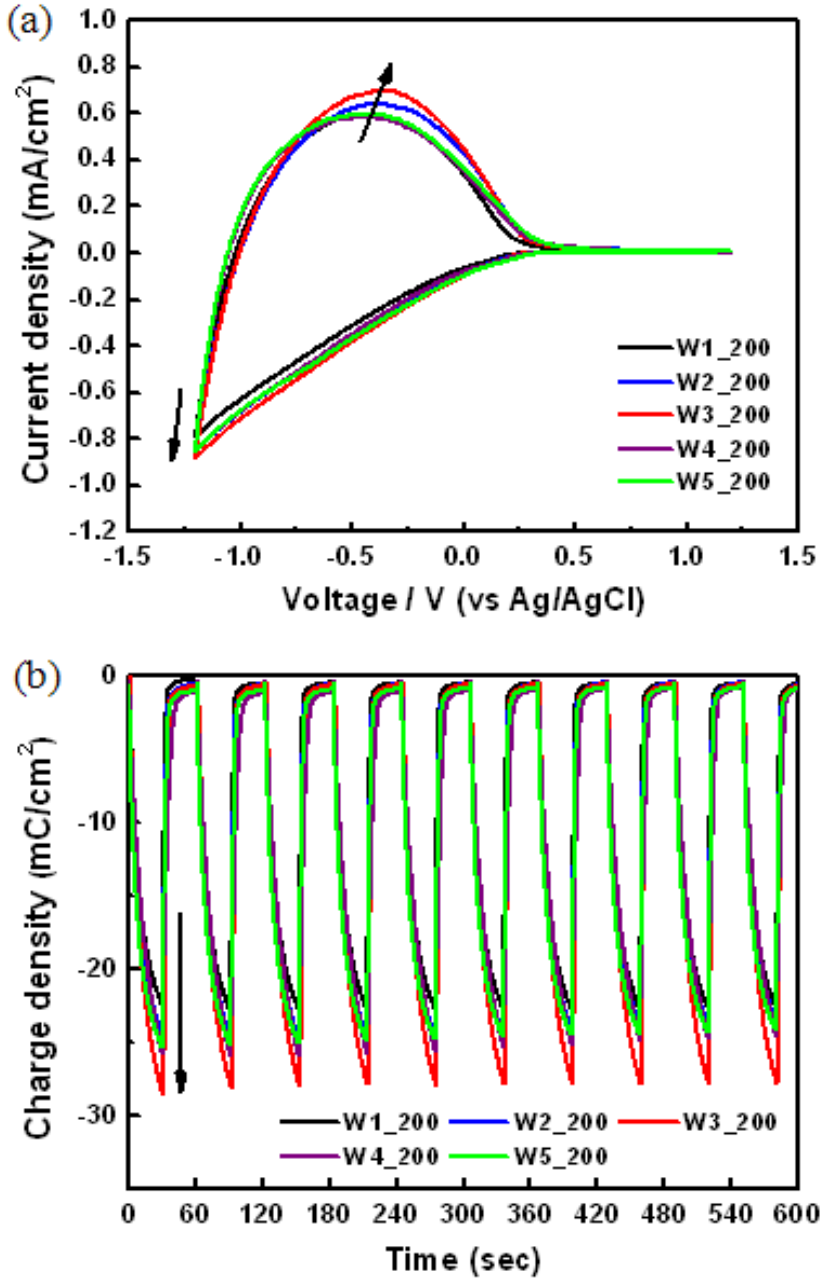

Figure 12. Electrochemical performance of WO_3 thin film with repeated coating; (a) cyclic voltammogram (CV) and (b) charge density (Q).

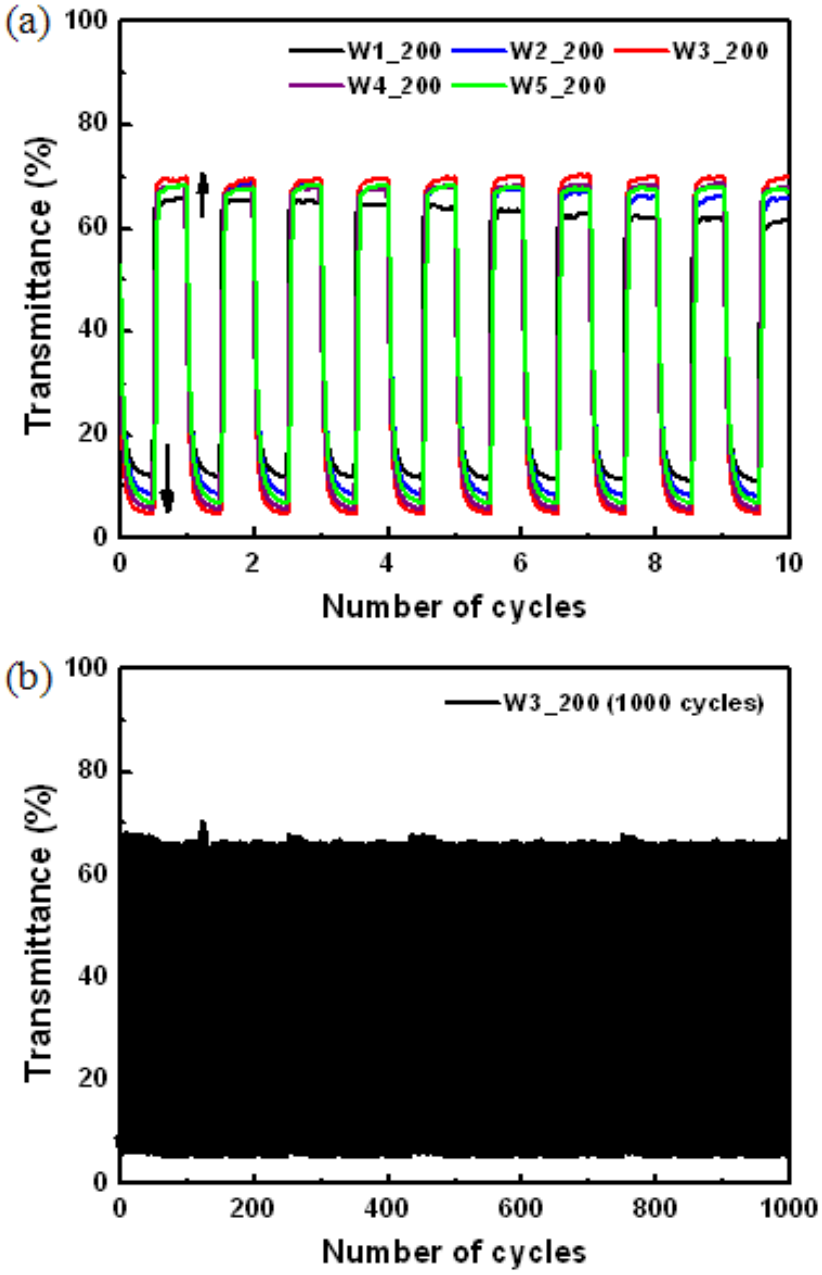

Figure 13. Optical properties of WO_3 thin film with repeated coating; (a) optical transmittance change (ΔT) and (b) long-term stability with continuous potential cycling.

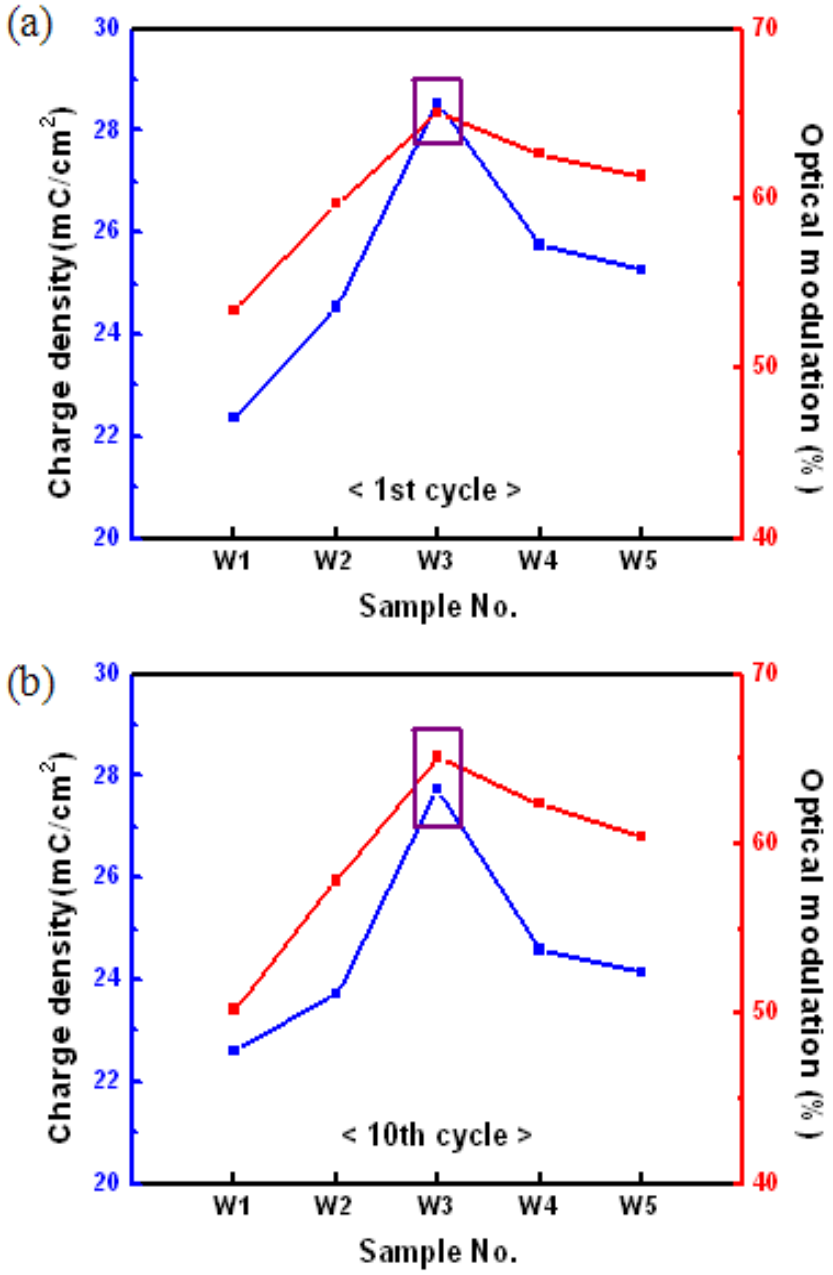

Figure 14. Comparison of charge density and optical modulation with repeated coating; (a) 1st cycle and (b) 10th cycle.

Sample No.		W1_200	W2_200	W3_200	W4_200	W5_200
Q (mC/cm^2)	1st	22.35	24.53	28.53	25.76	25.27
	10th	22.60	23.73	27.75	24.58	24.14
△OD(-)	1st	0.739	0.907	1.175	1.086	1.006
	10th	0.747	0.913	1.168	1.091	0.998
CE (cm^2/C)	1st	33.06	36.98	41.18	42.16	39.81
	10th	33.05	38.47	42.09	44.39	41.34

Table 2. Electrochromic properties of WO_3 thin film with repeated coating in half cell.

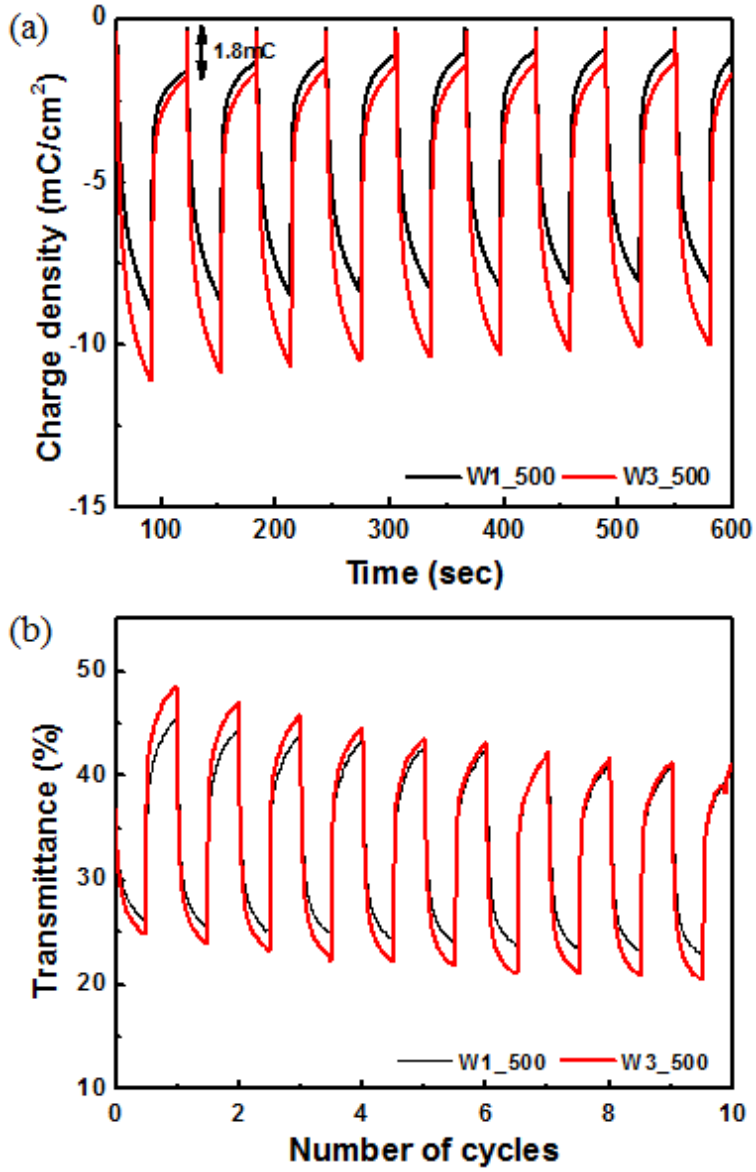

Figure 15. Electrochemical performance of WO_3 thin film annealed at 500 ℃; (a) charge density (Q) and (b) optical transmittance change (ΔT).

4.2 Photoelectrochromic characterization

4.2.1 Material analysis

To observing the effect of heat annealing at 200℃ and 500℃ on WO_3 thin film, XRD measurement was taken. As shown in Fig. 16(b), monoclinic WO_3 (JCPDS No.43-1035) peaks appeared after the heat annealing process at 500 ℃, indicating crystallization of WO_3 from amorphous phase obtained by heat annealing process at 200 ℃ (Fig. 16(a)).

In addition, in sample of layered structure as a photoanode, some extra peaks were observed except of monoclinic WO_3. These peaks represented the anatase phase of TiO_2 (JCPDS No.21-1272) from Fig. 16(c). These results noted that the WO_3 thin film was crystallized by sintering process of TiO_2 layer onto the WO_3 in photoanode. WO_3 had monoclinic crystalline phase and we confirmed that TiO_2 layer onto the WO_3 thin film for photoelectrochromic cell (layered structure) were successfully deposited.

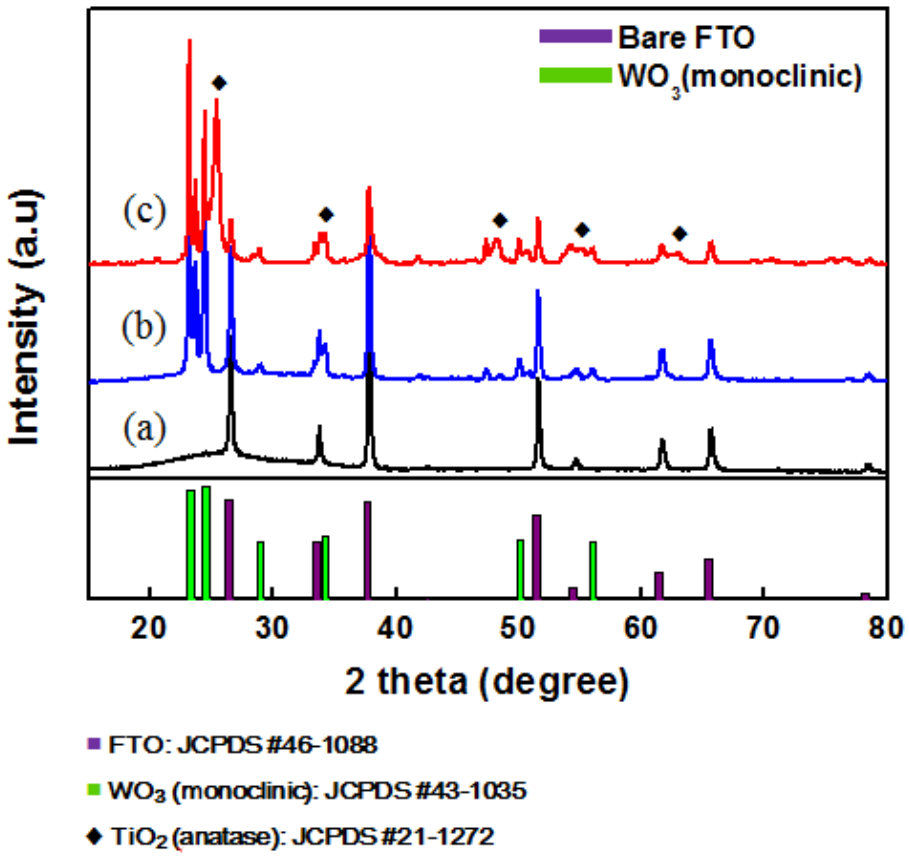

Figure 16. XRD patterns of (a) WO_3 thin film annealed at 200 ℃, (b) annealed at 500 ℃, and (c) TiO_2 layer on WO_3 thin film.

4.2.2 Optical properties

Fig. 17(a, b) represent the design of a two types of PECC that we applied for photoelectrochromic study. As explained to previous chapter, both photo-electrochromic systems were designed by combining the electrochromic device (ECD) and dye-sensitized solar cell (DSSC). In this kind of device, the electrochromic reaction can proceed without an external power source, because the power for coloration of electrochromic film was directly supplied from the DSSC part of PECC[11].

In contrast to that, clear difference between two systems was that if this device is exposed to light, in the case of separate structure, electrons are generated in the TiO_2 and are injected into the WO_3 via the external circuit. This leads to the coloration of the WO_3.

So, we employed the WO_3 thin film prepared by dip-coating method to two types of photoelectrochromic systems for observing optical transmittance kinetics as illumination time goes on and compared it with solely electrochromic optical properties in previous chapter.

We abbreviated each sample related to coating number (once as 1 and three-times coated as 3) and heat annealing process (200 ℃ as LT and 500 ℃ as HT) in two types of photoelectrochromic systems, layered (layered_1_HT, layered_3_HT) and separate structure (separate_1_LT,

separate_1_HT, Separate_3_LT, Separate_3_HT).

Fig. 18(a, b) and fig. 19(a-d) were shown transmittance spectra of the as prepared and colored state of PECCs after AM 1.5 illumination (100 mW/cm^2) for 1 - 30 min.

We could compare once-coated crystalline WO_3 thin film (1.1 μm) employed PECC with that of three-times coated thin film (460 nm) in layered structure in Fig 18(a). The optical transmittance changes were so small and exhibited slow coloration change kinetics for both sample, indicating that the WO_3 thin film in layered structure was performed to transfer electron to current collector from TiO_2 conduction band.

In other words, Li ions in liquid electrolyte were not well inserted in WO_3 matrix with electrons. Instead of that, electrons from the TiO_2 conduction band were moved just along the WO_3 conduction band pathway to current collector.

When compared three-times coated films employed PECC with that of once-coated, three-times coated films employed PECC exhibited slightly higher optical properties than once-coated film as illumination time goes on.

Transmittance spectra of PECC in separate structure were also shown fig. 19(a-d). Comparison fig. 19(a) with (c) and (b) with (d), we could understand the effect of the heat annealing process of WO_3 thin film. It showed

that the amorphous WO_3 employed PECC strongly exhibited higher optical transmittance properties with fast switching kinetics compared to that of crystalline WO_3 employed regardless of film thickness.

In addition, when compared fig. 19(a) with (b) and (c) with (d), thinner WO_3 film employed PECC (fig. 19(b, d)) exhibited the slightly fast switching kinetics after 1 min illumination especially. These results showed that in the case of photoelectochromic system, optical modulation changes exhibited same tendency compared to crystalline phase and film thickness dependent electrochromic properties.

Furthermore, WO_3 thin film in separated structure exhibited faster optical transmittance switching kinetics with illumination time than that of in layered structure from fig. 18(a, b) and fig. 19(a, b). These two samples, however, showed a poor optical properties compared to the amorphous WO_3 employed PECC in separate structure from fig. 19(c, d).

Table 3(a-c) was shown the absolute changing values of optical transmittance both layered and separate structure in PECC. In amorphous WO_3 employed PECC at separate structure in table 3(c), higher than 50% decrease in optical transmittance was exhibited just after 1 min illumination compared to as-prepared state.

It was believed that WO_3 thin film at separate structure in PECC was

performed almost as chromism by cation insertion with electrons from the photoanode via external circuit.

UV-vis optical transmittance change at 633 nm (visible region) was also shown in fig. 20 for observing that in visible region. As I mentioned from fig. 18 and fig. 19, this gave us same meaning that amorphous WO_3 thin film employed PECC in separate structure exhibited the fast coloration kinetics compared to others

However, when compared as-prepared state with final state of PECC, absolute values of optical transmittance changes were almost same in both structures even if film thickness was different. It is believed that because PECCs in this study used the ruthenium based dye having red color.

Therefore, we could observe the gradual color change of PECCs from red color at as-prepared state to dark black color as illuminated time goes on.

In overall, UV-vis optical transmittance test results showed same tendency compared to crystalline phase and film thickness dependent electrochromic properties from previous chapter and we could also observe that separate structure in PECC exhibited better optical property than layered structure.

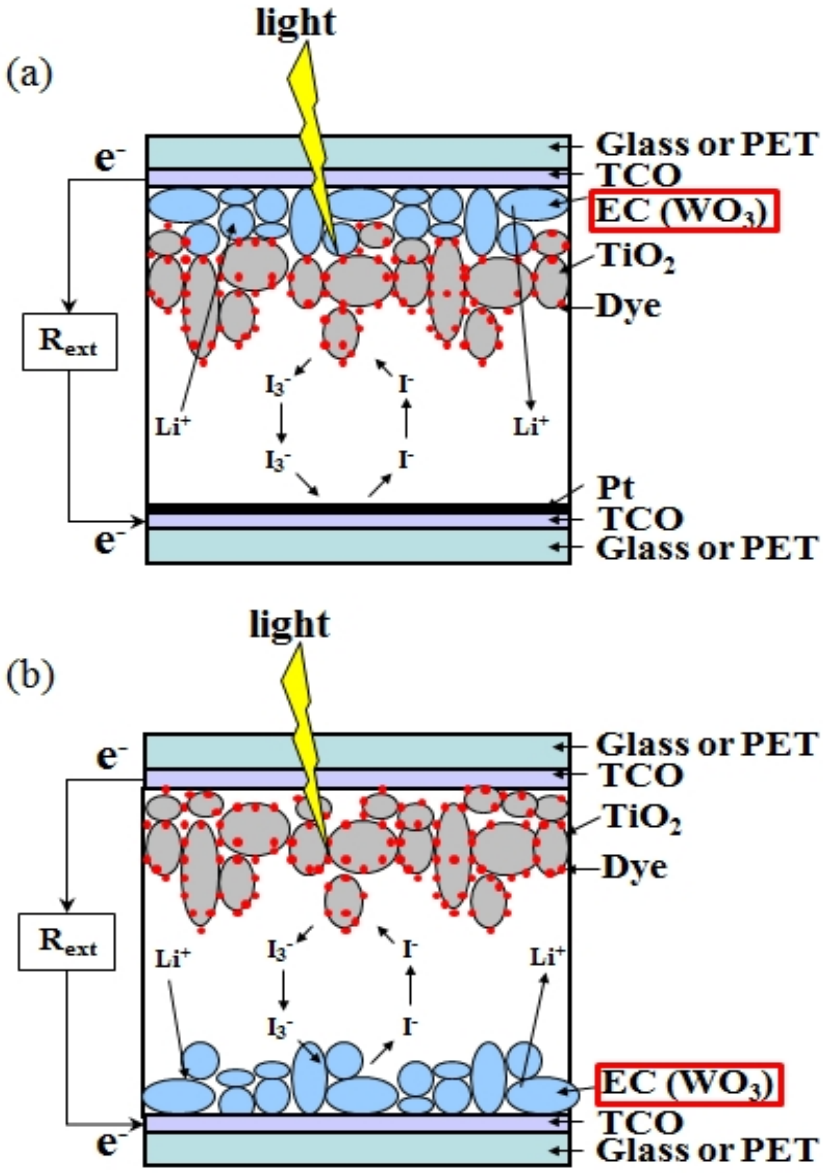

Figure 17. The design of the photoelectrochromic systems; (a) layered structure and (b) separate structure.

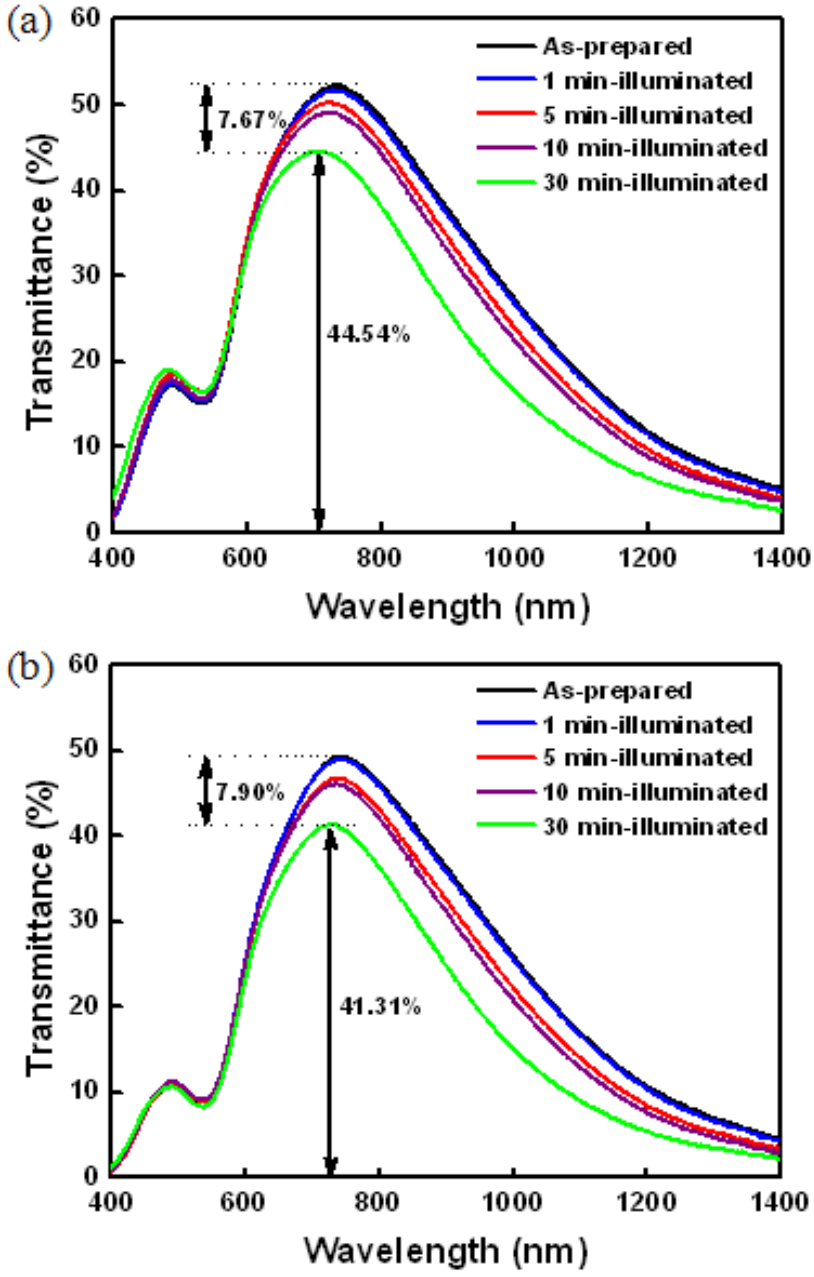

Figure 18. UV-vis transmittance spectra in layered structure; (a) layered_1_HT and (b) layered_3_HT.

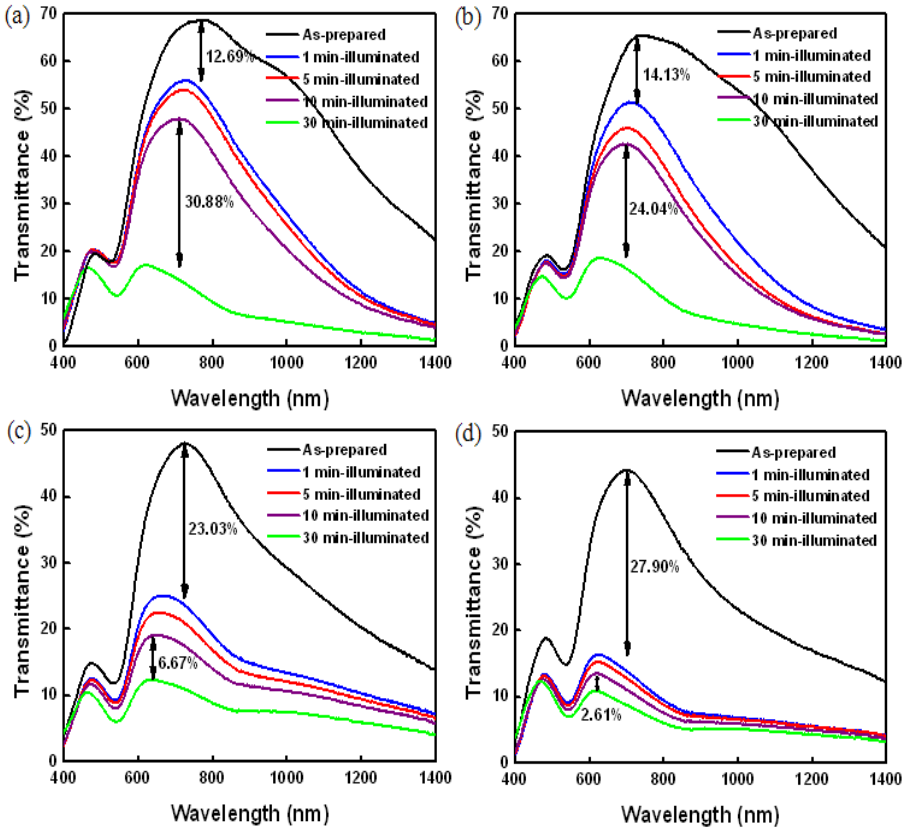

Figure 19. UV-vis transmittance spectra in separate structure; (a) separate_1_HT, (b) separate_3_HT, (c) separate_1_LT, and (d) separate_3_LT.

(a)

Sample No.		Layered_1_HT		Layered_3_HT	
		Wavelength (nm)	T (%)	Wavelength (nm)	T (%)
As-prepared		738	52.21	740	49.21
30 min-illuminated		706	44.54	728	41.31
Shift (nm)	Decay (%)	32	7.67 (14.70%)	12	7.90 (16.05%)

< Layered-structure >

(b)

Sample No.	Separate_1_HT		Separate_3_HT	
	Wavelength (nm)	T (%)	Wavelength (nm)	T (%)
As-prepared	775	68.80	744	65.59
1 min-illuminated	726	56.11 (18.44%)	713	51.46 (21.54%)
10 min-illuminated	707	47.97	691	42.62
30 min-illuminated	620	17.08 (64.37%)	627	18.58 (56.40%)

(c)

Sample No.	Separate_1_LT		Separate_3_LT	
	Wavelength (nm)	T (%)	Wavelength (nm)	T (%)
As-prepared	729	48.05	700	44.26
1 min-illuminated	660	25.02	627	16.36
Shift (nm) Decay (%)	69	23.03 (47.93%)	73	27.90 (63.04%)

< Separate-structure >

Table 3. UV-vis transmittance change in (a) layered structure and (b), (c) separate structure.

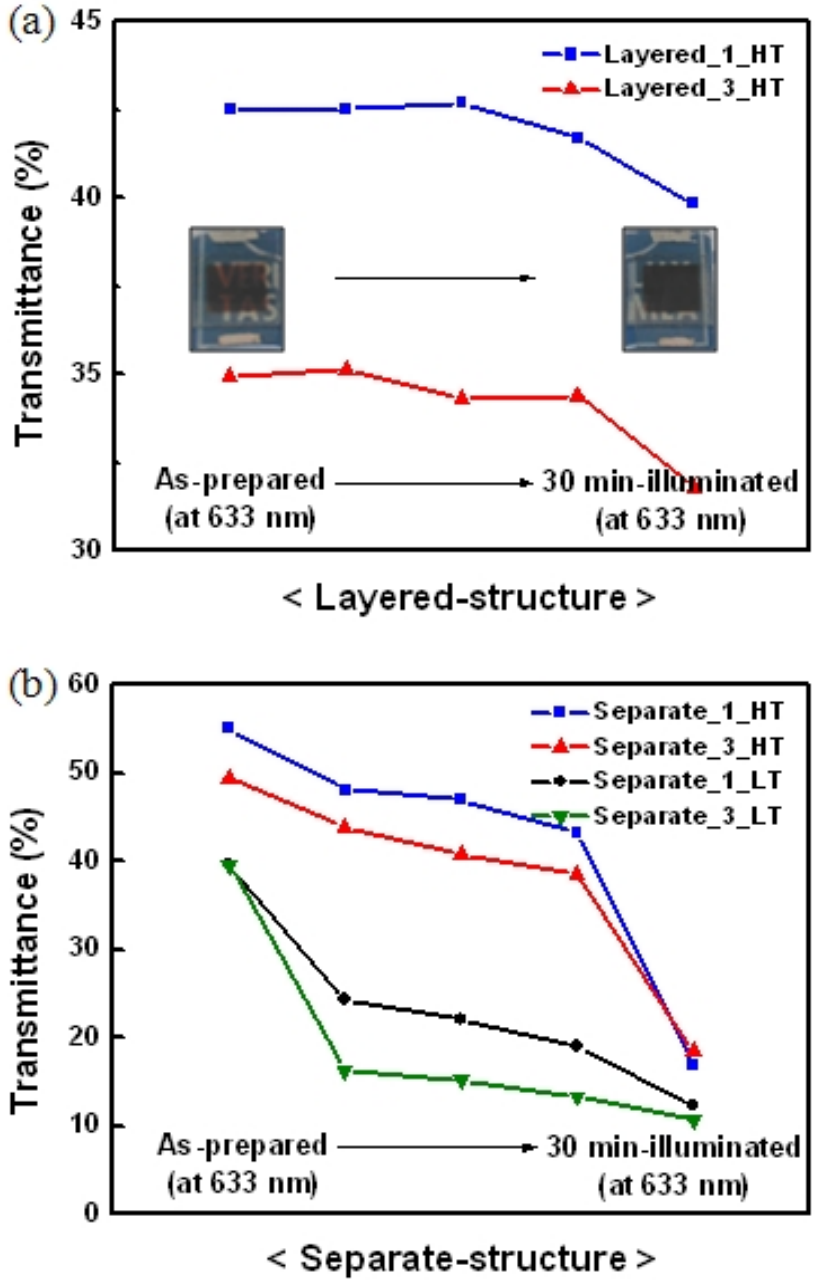

Figure 20. UV-vis transmittance change at 633 nm (visible region) in (a) layered structure and (b) separate structure.

Chapter 5. Conclusions

In this study, the electrochromic WO_3 thin film was fabricated by sol-gel dip-coating method and heat annealed at 200℃ to transfer from $W(OH)_6$ to WO_3 by evaporating water. We confirmed the amorphous phase of WO_3 via XRD measurement. In addition, we observed good film adhesion with substrate after heat annealing process and thickness changing tendency for WO_3 thin film by repeated dip-coating were also observed by FE-SEM cross-sectional images.

All samples with different coating number were electrochemically evaluated by cyclic voltammogram and continuous potential cycling test in lithium-based electrolyte. Three-times coated film had the largest capacity and degradation of optical transmittance change was noted less than 3% even after 1,000 cycles of continuous potential cycling, which means long-term stability of this film was quite good. So, we decided the electrochromic film exhibiting best electrochromic properties and once coated film as control group for employing the two types of photoelectrochromic systems.

UV-vis optical transmittance test results showed WO_3 of thinner film with amorphous phases in separated structure exhibited the best coloration switching kinetics compared to others as illuminated times goes on.

Furthermore, absolute optical transmittance changes value also quite remarkable. It would mean that the photoelectrochromic system in separate structure, WO_3 thin film performed almost as a chromic by cation insertion with electrons from the photoanode via external circuit.

In other words, iodine was not well transferred triiodide by accepting electrons followed by dye regeneration in photoelectrochromic system. In layered structure, however, which TiO_2 layer is on the WO_3 film, Li ions in liquid electrolyte were not inserted well in WO_3 host matrix with electrons because WO_3 thin film performed as electron transfer pathway from TiO_2 conduction band edge to current collector. Therefore, WO_3 thin film in layered structure exhibited poor electrochromic properties than in separate structure.

In overall, we fabricated the WO_3 electrochromic thin film by sol-gel dip-coating method and these films were applied two types of photoelectro-chromic systems. We could observe that two photoelectrochromic systems exhibited same tendency compared to crystalline phase and film thickness dependent electrochromic properties and we could also observe that separate structure in PECC exhibited better optical property than layered structure from the UV-vis optical transmittance test results.

In addition, when compared as-prepared state with final state of PECC,

absolute values of optical transmittance changes were almost same in both structures even if film thickness was different because we used the ruthenium based dye having red color in this study.

So, for enhancing the optical properties of photoelectrochromic systems, which were dip-coated WO_3 electrochromic thin film was employed, more transparent dyes on TiO_2 NP have to be used for higher transmittance value at initial state (as-prepared state) in two types of photo-electrochromic systems.

References

[1] P. R. Somani, S. Radhakrishnan, "Electrochromic materials and devices: Present and future", *Mater. Chem. Phys.*, **77**, 117 (2002).

[2] P. M. S. Monk, R. J. Mortimer, D. R. Rosseinsky, "Electrochromism: Fundamentals and Applications", 1995.

[3] R. D. Rauh, "Electrochromic windows: an overview", *Electrochim. Acta*, **44**, 3165 (1999).

[4] C. G. Granqvist, A. Azens, A. Hjelm, L. Kullman, G. A. Niklasson, D. Ronnow, M. S. Mattsson, M. Veszelei, G. Vaivars, "Recent advances in electrochromics for smart windows applications", *Solar energy*, **63**, 199 (1998).

[5] D. R. Rosseinsky, R. J. Mortimer, "Electrochromic Systems and the prospects for devices", *Adv. Mater.*, **13**, 783 (2001).

[6] J. L. Garcia-Miquel, Q. Zhang, S. J. Allen, A. Rougier, A. Blyr, H. O. Davies, A. C. Jones, T. J. Leedham, P. A. Williams, S. A. Impey, "Nickel oxide sol–gel films from nickel diacetate for electrochromic applications", *Thin Solid Films*, **424**, 165 (2003).

[7] P. M. S. Monk, R. J. Mortimer, D. R. Rosseinsky, "Electrochromism and electrochromic devices", 1995.

[8] C. G. Granqvist, “Handbook of inorganic electrochromic materials”, 1995.

[9] K. Wang, P. Zeng, J. Zhai, Q. Liu, “Electrochromic films with a stacked structure of WO_3 nanosheets”, *Electrochem. Commun*., **26**, 5 (2013).

[10] C. Beshinger, S. Ferrere, A. Zaban, J. Sprague, B. A. Gregg, “Photoelectrochromic windows and displays”, *Nature*, **383**, 608 (1996).

[11] A. Hauch, A. Georg, S. Baumgartner, U. O. Krasovec, B. Orel, “New photoelectronchromic device”, *Electrochim. Acta*, **46**, 2131 (2001).

[12] J. -J. Wu, M. -D. Hsieh, W. -P. Liao, W. -T. Wu, J. -S. Chen, “Fast-switching photovoltachromic cells with tunable transmittance”, *ACS Nano*, **3**, 2297 (2009).

[13] C. Santato, M. Odziemkowski, M. Ulmann, J. Augustynski, “Crystallographically oriented mesoporous WO_3 films: Synthesis, characterization and applications”, *J. Am. Chem. Soc.*, **123**, 10639 (2001).

[14] F. Lin, J. Cheng, C. Engtrakul, A. C. Dillon, D. Nordlund, R. G. Moore, T. -C. Weng, S. K. R. Williams, R. M. Richards, “In situ crystallization of high performing WO_3-based electrochromic materials and the importance for durability and switching kinetics”, *J. Mater. Chem*., **22**, 16817 (2012).

[15] C. J. Brinker, G. C. Frye, A. J. Hurd, C. S. Ashley, "Fundamentals of sol-gel dip coating", *Thin Solid Films,* **201**, 97 (1991).

[16] J. D. Wright, N.A.J.M. Sommerd, "Sol-gel materials: Chemistry and applications", 2001.

[17] B. E. Yoldas, D. P. Partlow, "Formation of broad band antireflective coatings on fused silica for high power laser applications", *Thin Solid Films*, **129**, l (1985).

[18] B. Orel, U. O. Krasovec, M. Mace, F. Sveg, U. L. Stangar, "Comparative studies of all sol–gel electrochromic devices with optically passive counter-electrode films, ormolyte Li^+ ion-conductor and WO_3 or Nb_2O_5 electrochromic films", *Sol. Energy Mater. Sol. Cells*, **56**, 343 (1999).

[19] P. Judeinstein, J. Livage, "Sol-gel synthesis of WO_3 thin films", *J. Mater. Chem.*, **1**, 621 (1991).

[20] M. Deepa, T. K. Saxena, D. P. Singh, K. N. Sood, S. A. Agnihotry, "Spin coated versus dip coated electrochromic tungsten oxide films: Structure, morphology, optical and electrochemical properties", *Electrochim. Acta*, **51**, 1974 (2006).

[21] J. Huang, R. Fan, S. Connor, P. Yang, "One-step patterning of aligned nanowire arrays by programmed dip coating", *Angew. Chem.*, **119**, 2466 (2007).

[22] Y. Lu, R. Ganguli, C. A. Drewien, M. T. Anderson, C. J. Brinker, W. Gong, Y. Guo, H. Soyez, B. Dunn, M. H. Huang, J. I. Zink, "Continuous formation of supported cubic and hexagonal mesoporous films by sol–gel dip-coating", *Nature*, **389**, 25 (1997).

[23] Y. C. Nah, A. Ghicov, D. Kim, S. Berger, P. Schmuki, "TiO_2-WO_3 composite nanotubes by alloy anodization: Growth and enhanced electrochromic properties", *J. Am. Chem. Soc.*, **130**, 16154 (2008).

초 록

스마트 창문으로 적용할 수 있는 가장 일반적인 재료가 외부 전압의 인가나 빛의 조사에 따라 가역적으로 투과율이 변하는 전기변색과 광변색 물질이다. 이의 대안으로 광전기변색 재료가 1996년에 보고되었는데 외부의 전압인가 없이 내부에서의 광자의 전자 변환으로 변색이 될 수 있는 장점이 있다.

본 연구에서는 졸겔법 딥 코팅의 반복적인 공정을 이용하여 전기변색 박막의 두께를 조절하였고, 두 가지 온도의 열처리를 통하여 전기변색 박막의 성능 차이를 평가하였다. 1몰 $LiClO_4$/PC 전해질 내에서 3전극 시스템을 이용하여 반쪽 전지의 전기화학 테스트와 He-Ne 레이저(633 nm)를 이용하여 착색/소색 상태의 광학 투과율 측정을 수행하였다.

그리고 딥 코팅 방법으로 만든 전기변색 박막을 두 가지 형태의 광전기변색 시스템에 적용하여 빛의 조사 시간에 따른 투과율 특성 변화를 측정하였고, 이를 앞서 측정한 박막 두께와 열처리 온도에 따른 전기변색 박막 성능의 경향성과 비교하여 보았다.

전기변색 박막의 재료분석 결과, 열처리 과정을 거친 텅스텐 옥사이드 전기변색 박막이 인듐-주석 기판과의 접착이 우수하였고, 딥 코팅 공정을 반복할수록 박막 두께가 감소하는 경향을 보였다.

또한 비결정 구조를 가지는 박막이 결정성을 가지는 박막보다 전기변색 성능이 우수하였으며, 광전기변색 시스템에 적용하기 위한 전기변색 성능이 가장 우수한 최적의 전기변색 박막 두께를 결정할 수 있었다.

앞선 딥 코팅 방법으로 만든 텅스텐 옥사이드 박막 중 가장 전기변색 성능이 우수한 박막과 이의 대조군으로 딥코팅 공정을 1번 거친 박막을 선정하여 이를 두 가지 구조의 광전기변색 셀에 도입하였다. 하나는 결정화된 텅스텐 옥사이드 박막 위에 타이타늄 옥사이드 층이 올라간 형태의 음극과 백금을 양극으로 사용한 층상 구조이고, 다른 하나는 비정질 또는 결정화된 텅스텐 옥사이드를 양극으로 사용하고, 염료가 흡착된 타이타늄 옥사이드를 음극으로 사용한 분리된 구조이다.

투과율 특성 측정 결과, 비결정 구조이고 두께가 얇은 텅스텐 옥사이드 전기변색 박막을 도입한 분리된 구조의 광전기변색 셀에서 빛의 조사 시간에 따라 가장 우수한 투과율 변화 특성을 보였고, 그 값도 상당하였다. 또한, 결정화된 텅스텐 옥사이드 박막을 도입한 층상 구조의 셀보다 동일한 박막을 도입한 분리된 구조의 셀이 좀 더 향상된 성능을 나타내었다.

이 결과는 앞선 텅스텐 옥사이드의 열처리 온도에 의한 결정성 유무와 박막 두께에 따른 전기변색 성능 평가 결과와 일치함을

보여줌으로써 딥 코팅 방법으로 만든 전기변색 박막을 광전기변색 시스템으로 도입하였을 때에도 빛의 조사 시간에 따른 투과율의 변화 속도 특성의 경향성은 동일하다는 것을 나타낸다.

그러나 초기 상태와 최종 상태의 투과율의 차이는 두 가지 구조의 광전기변색 셀에서 박막 두께와 결정성 유무에 관계없이 비슷한 수치를 나타내는 점으로 미루어 보았을 때, 광전기변색 셀에서 전기변색 박막의 초기 투과율 성능의 향상을 위해서는 사용되는 염료의 투명성 확보가 무엇보다 중요한 요소임을 본 연구를 통하여 본인에게 암시하여 주었다.

주요어: 텅스텐 옥사이드, 딥 코팅, 광전기변색 시스템

학 번: 2012-23977